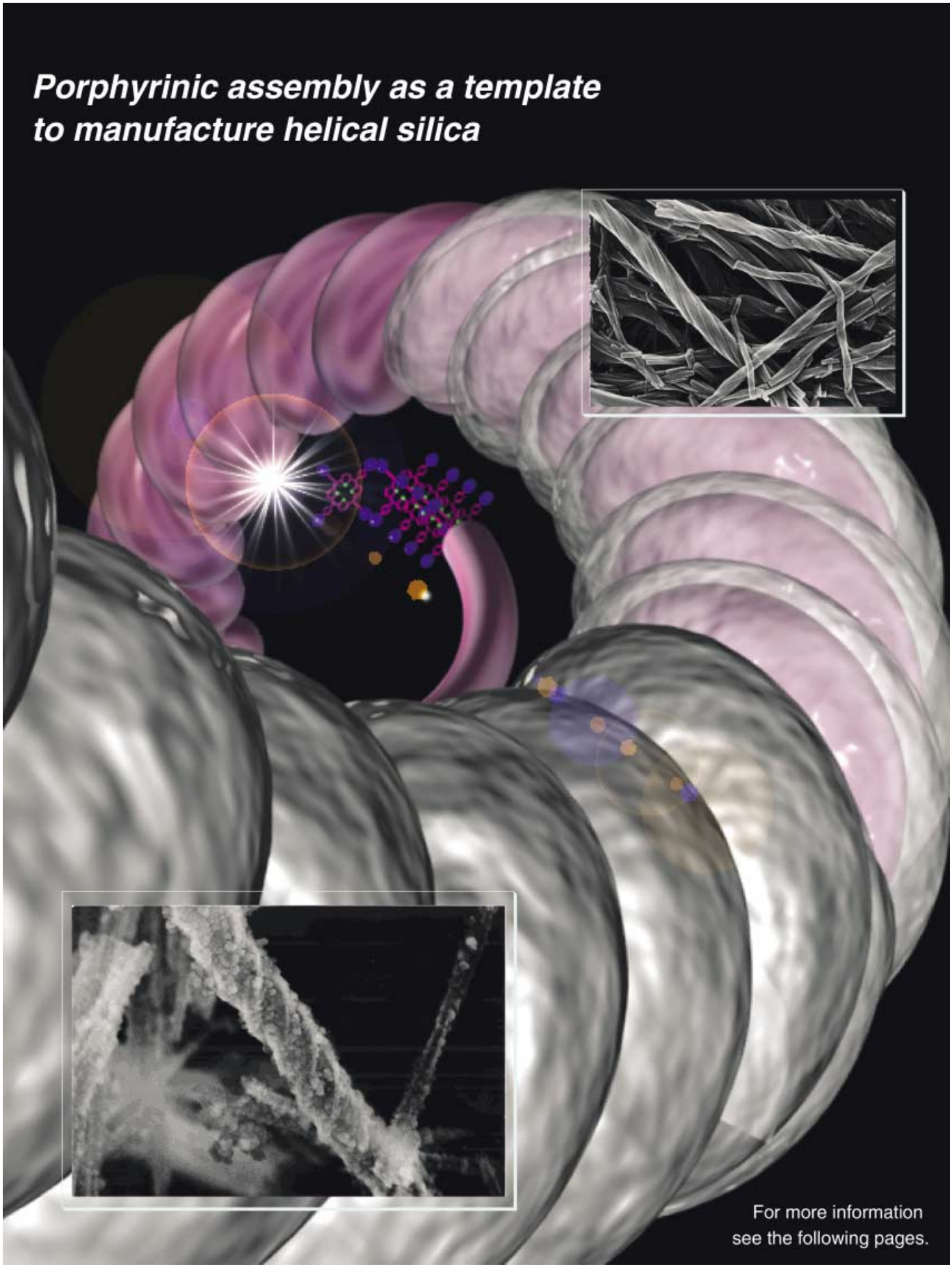

 DOI: 10.1002/chem.200305042

Sol–Gel Polycondensation of Tetraethyl Orthosilicate (TEOS) in Sugar-Based Porphyrin Organogels: Inorganic Conversion of a Sugar-Directed Porphyrinic Fiber Library through Sol–Gel Transcription Processes

Shin-ichiro Kawano,[a] Shun-ichi Tamaru,[b] Norifumi Fujita,[a] and Seiji Shinkai*[a]

Abstract: Sugar-appended porphyrins (**1a**–**e**) with monosaccharide groups at their periphery have been rationally designed for a new class of gelating reagents. A few of these compounds have the tendancy to form one-dimensional aggregates stable enough to show successful gelation ability for DMF–alcohol mixed solvents. The aggregation mode in the specific columnar super structures has been evaluated in detail by UV-visible spectrometry (UV/Vis), circular dichroism (CD), scanning electron microscopy (SEM), and transmission electron microscopy (TEM). All UV-visible spectra of sugar-appended porphyrinic gels obtained from **1a**–**c** exhibit Soret band absorptions, which shift to lower wavelength and are significantly broadened. This phenomenon indicates that these porphyrin cores strongly interact with each other in an H-aggregate fashion, which drives the generation of a one-dimensional porphyrin-stacking array. The CD spectra of the organogels from **1a** and **1b**, which are in anomers, exhibit an almost symmetric pattern, whereas the gel from **1c** gives a completely different pattern. This implies that the gel fibrils wind themselves in a right- or left-handed fashion; this reflects chirality in the specific molecular structure of the gelators. The results from SEM for the gel fibrils are in good agreement with the CD patterns. The gel fibrils in **1a** possess left-handed helicity, whereas those in **1b** wind themselves right-handedly. Macroscopic helical morphology reflects the microscopic structure well at a molecular level, which gives structural variety of the gel fibrils, which can be defined by the sugar library. Inorganic conversion of the organic helical fibrils by a sol–gel transcription process successfully gives the helical-silica structures, which finely inherit the organic morphology. A striking observation is that a unimolecular porphyrin-stacking array is also transcribed into silica fibers when the optimized sol–gel reaction conditions are selected. A sugar-based organic-fiber library in porphyrinic gels thus provides a variety of inorganic materials through the sol–gel transcription process.

Keywords: helical structures · organogels · porphyrinoids · silicates · sol–gel processes

Introduction

One-dimensional alignment of porphyrins and phthalocyanines is of much concern in relation to the creation of novel supramolecular architectures such as nanowires, discotic liquid crystals, helical ribbon structures, and so on.[1–5] The major driving force of these structures is considered to be a π–π interaction. More recently, other supramolecular architectures constructed in organogels have attracted the widely spread attention of supramolecular chemists, and the origin of organogel formation is considered to be a one-dimensional alignment of gelator molecules supported by van der Waals interactions and/or hydrogen-bonding interactions.[6,7] This concept presents a new theory for porphyrins and phthalocyanines, in that they could act as powerful building blocks for the design of a new gelator, whereas before, theses compounds tended to assemble into a one-dimensional supramolecular architecture. In addition, we found that many new hydrogen-bond-based gelators can be developed by using a natural library of carbohydrate molecules.[8,9] In a few cases, the solvents were gelated by the presence of only 0.3–0.5 g dm^{-3} sugar-based gelators.[10] The findings suggest that one-dimensional aggregates composed of porphyrins or phthalocyanines were "reinforced" by the hydrogen-bonding

[a] S.-i. Kawano, Dr. N. Fujita, Prof. Dr. S. Shinkai
Department of Chemistry & Biochemisry
Graduate School of Engineering, Kyushu University
6-10-1 Hakozaki, Higashi-ku
Fukuoka 812-8581 (Japan)
Fax: (+81) 92-642-3611
E-mail: seijitcm@mbox.nc.kyushu-u.ac.jp

[b] Dr. S.-i. Tamaru
Department of Chemistry
North Carolina State University
Campus Box 8204, Raleigh NC
27695–8204 (USA)

Supporting information for this article is available on the WWW under http://www.chemeurj.org/ or from the author.

DOI: 10.1002/chem.200305042

interaction among saccharide groups covalently-appended to the central porphyrins (or phthalocyanines) column. However, this idea has scarcely been used for the design of a robust organogel system.[11] It thus occurred to us that porphyrin molecules, the periphery of which is modified with saccharide groups, formed a one-dimensional aggregate as a result of the synergistic effect of porphyrin–porphyrin π–π stacking and saccharide–saccharide hydrogen-bonding interactions; this eventually resulted in the formation of stable organogels (Scheme 1).[12,13] With this in mind, we synthesized porphyrins **1a–e**, that bear four saccharide groups at their periphery. They form helical aggregates in gel, that are indeed different from the aggregate made of the gelator reported in the former paper.[12] Moreover, we have now found that the helicity of one-dimensional aggregates is precisely consistent with the chirality in the saccharide moieties of the gelators, and as is shown in this paper, the CD spectroscopic analyses are also in good agreement with them. Thus, the first new aspect that we have established is the creation of various gel superstructures, which arise from saccharide structures. Previously, we have shown that these kind of "organic" superstructures can be elaborately transcribed into "inorganic" silica materials by using template–silanol interactions.[14] By using this methodology, we have succeeded in discovering that a family of sugar-appended porphyrin gelators, that offer unique helical superstructures in the organogels, can act as templates for silica gel mineralization. The sol–gel transcription applied to this gel system with tetraethylorthosilicate (TEOS) has provided a series of helical silica-coated porphyrin fiber libraries, which finely inherit the tissue morphology of the organogels. This is the second new aspect we have established in this work. Interestingly, we noticed that the rate of bundle growth of this gelator is relatively slow, which provides us with a greater chance to transcribe nanosized incipient fibers into silica. In fact, we have found that a hollow silica-fiber with an inner diameter of 4–5 nm is created, and can be compared to the length of the long axis in **1a.** This is a rare example of a unimolecular stack of porphyrins immobilized in an inorganic material.

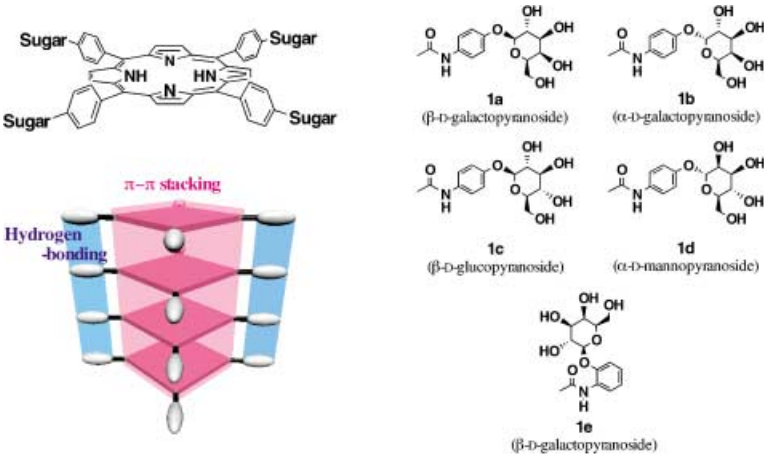

Scheme 1. Molecular structure of the sugar-appended porphyrins and a schematic representation of the one-dimensional porphyrin stacking structure supported by binary domain, π–π stacking, and hydrogen-bonding.

Results and Discussion

Syntheses of sugar-appended porphyrins: Sugar-appended porphyrin compounds, **1a–e** were synthesized in accordance with Scheme 2. Aminophenyl-2,3,4,6-tetra-*O*-acetyl monosaccharides[15] **3a–e** were obtained by the reduction of acetyl-protected nitrophenyl analogues **2a–e,** which were derived from corresponding nitrophenyl monosaccharides. Compounds **5a–e** were thus obtained by a condensation reaction with an acid-chloride derivative (**4**), which was derived from a benzoic-acid-appended porphyrin. Due to the deprotection of the hydroxyl groups, the porphyrins **1a–e** had monosaccharide groups at their periphery.

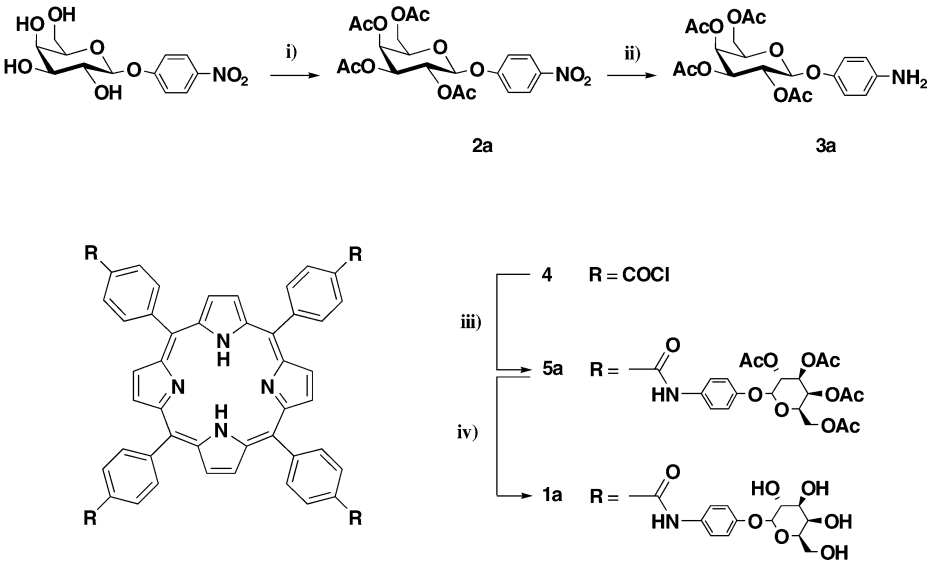

Scheme 2. Synthesis of the sugar-appended porphyrin **1a**. Conditions: i) Ac_2O, pyridine; ii) Pd/C, H_2, AcOEt; iii) **3a**, TEA, THF; iv) CH_3ONa, MeOH, THF. Compounds **1b–e** are synthesized according to the same strategy.

Gelation property: The gelation property of **1a–e** was tested for 21 solvents (at 30 g dm^{-3}), which ranged from water, alcohols, and dipolor aprotic solvents to aromatic solvents and hydrocarbon solvents (see footnote a in Table 1). None of the solvents could be gelated by compounds **1a–e** because of their poor solubility. This poor solubility seems to be associated with the intrinsic feature of sugar-appended porphyrins, that is, the strong self-association tendency, that arises from the strong π–π interaction between the porphyrin π-planes and the intermolecular multi hydrogen-bonding interactions between hydroxy groups in the saccharides.

To overcome this problem, we screened many solvents and eventually found that *N*,*N*-dimethylformamide (DMF) can dissolve compounds **1a–e** very well. We expect, therefore, that once **1a–e** are dissolved in a good solvent (i.e., DMF) in order to dissociate the strong intermolecular interaction, there is a possibility to form one-dimensional columnar aggregates with the aid of a moderate interaction by the addition of a poor solvent. Indeed, the gelation properties of **1a–e** were generated by this stepwise process as follows. The gelators were dissolved in DMF in a capped test-tube followed by the addition of a poor solvent (30 g dm^{-3}, DMF/poor solvent 1:3 (*v*/*v*)). The resulting solutions were heated and then left at room temperature. The sample vials were cooled in air to 25 °C, left for 1 h, and then turned upside down. By immobilizing the solvent at this stage, the gelator formed a clear or slightly opaque gel; this is denoted as "G" in Table 1. The gelation property of **1a–e** was tested for eight kinds of DMF-based mixed solvents according to the procedure stated above. As shown in Table 1, **1a** and **1c** gelated well when mixed solvents with alcohols were used, and **1b** also gelated a DMF–benzylalcohol mixed solvent. This gelation behavior is probably due to the balance of intermolecular interactions versus solubilization, since the alcohol solvents prevent the gelators from growing into a thick bundle. Compound **1d**, however, did not possess a high gelation ability, and formed partial gels with alcohols even in a higher concentration of **1d** or in a higher ratio of poor solvents. Compound **1e** did not work as a gelator for any mixed solvents tested herein, because of its high solubility. It is interesting that a slight change in sugar structure drastically affects the solubility and the aggregation mode. Hereafter, we subjected **1a**, **1b**, and **1c**, that acted as gelators to the subsequent analyses.

One can improve the gelation properties of physical gels when the concentration of gelator is increased. We estimated the concentration dependency of gel–sol-phase transition temperature (T_{gel}) for the **1a–c** gels prepared from DMF/benzylalcohol 1:3 (*v*/*v*) mixed solvent. All gels show similar dependency, that is, T_{gel} increases with an increase in gelator concentrations (Figure S1: see Supporting information). Notably, the gels from **1a** ([**1a**] > 18 g dm^{-3}) and **1c** ([**1c**] > 9.0 g dm^{-3}) possess a high T_{gel}, which is above the boiling point of DMF (153 °C). The CGCs (critical gelation concentrations) of the gels in the mixed solvent (DMF/benzylalcohol 1:3 (*v*/*v*)) from **1a**, **1b**, and **1c** were determined to be 5.0 g dm^{-3}, 4.0 g dm^{-3}, and 3.0 g dm^{-3}, respectively; this was obtained by extrapolating the curves in Figure S1 in the Supporting Information. As stated above, the gels of the mixed solvent from **1a**, **1b**, and **1c** show a higher thermostability than the boiling point of DMF. The gels also show high gelation ability, which is called a "supergelator".[10]

Gelation is also affected by the ratio of DMF and benzylalcohol (Table S1 in the Supporting Information). Compound **1a** can gel the mixed solvent (DMF/benzylalcohol 1:19 (*v*/*v*)), in which [**1a**] is 1.0 g dm^{-3} (T_{gel} = 32 °C). At this concentration, **1a** cannot gel the mixed solvents at a ratio of DMF/benzylalcohol 1:6 ~1:4 (*v*/*v*), in which the viscosity is decreased with an increase in the DMF ratio. At higher gelator concentrations, the gelation region becomes wider relative to the mixing ratios of the solvents. When the gelator concentration is set at 14 g dm^{-3}, a stable gel is formed in the ratio of the mixed solvents between 1:6 and 1:3 (v/v), the maximum T_{gel} being 153 °C at 1:5 (v/v). At higher concentrations (30 g dm^{-3}), **1a** forms precipitates in the region between 1:19 to 1:3 (v/v), and the gel is formed only in 1:2 (v/v) solvent. The same analyses were applied to **1b** and **1c** with their concentration fixed at 14 g dm^{-3}. When T_{gel} for **1a**, **1b**, and **1c** gels are plotted against the ratio of DMF–benzylalcohol mixed solvents, one can conclude that **1a** can gel the mixed solvents only in the ratio between 1:6 and 1:3 (*v*/*v*), **1b** and **1c** can gel them with the ratio as small as 1:39

Table 1. Gelation properties of the compounds **1a-e** for DMF-based mixed solvents at room temperature.[a,b]

Poor solvent	State[c]				
	1a	**1b**	**1c**	**1d**	**1e**
methanol	G	PG	G	PG	S
ethanol	G	P	G	PG	S
2-propanol	G	P	G	PG	S
1-butanol	G	P	G	P	S
benzylalcohol	G	G	G	PG	S
benzene	I	I	I	I	S
chloroform	I	I	I	I	S
water	I	I	I	I	S

[a] Tested 21 kinds of solvents systems are not gelated: water, methanol, ethanol, 2-propanol, 1-butanol, benzylalcohol, acetonitrile, hexane, cyclohexane, decahydronaphthalene, cyclohexanone, ethyl acetate benzene, toluene, *p*-xylene, anisol, diethyl ether, tetrahydrofuran, 1,4-dioxane, dichloromethane, chlorofolm, *N*,*N*′-dimethylformamide, dimethylsulfoxide, chlorofolm:methanol = 1:1. [b] DMF/poor solvent 1:3, in which the concentration of the compound is 30 g dm^{-3}. [c] G: gel, PG: partial gel, P: precipitation, S: homogenious solution, I: insoluble when heated.

(*v*/*v*) (Figure S2 in the Supporting Information). These facts shed light on the following mechanistic analyses on a molecular level.

As stated before, gelation is prevented by two- and three-dimensional growth of columnar aggregates, that arise from an intercolumnar interaction.[6,10] The strength of this intercolumnar interaction should reflect the molecular structure of peripheral sugar groups. It is known that the axial OH tends to form an intramolecular hydrogen bond, whereas the equatorial OH tends to form an intermolecular hydrogen bond.[8,9] Compound **1a** has one axial OH group and two equatorial OH groups, whereas the three OH groups in **1c** are all equatorial. The fact that **1c** can gel in a wider mixing ratio of DMF–benzylalcohol solvents than **1a,** suggests that the equatorial groups in **1c** work efficiently to stabilize the hydrogen-bonding network.

UV-visible spectroscopic analyses: Figure 1 shows the UV-Visible absorption spectra for **1a–c**. The absorption spectrum of DMF solution of **1a** (2.3×10^{-6} M) gives the Soret band at 422 nm, and the Q bands at 517, 553, 593, and 647 nm. When **1a** (3.9×10^{-3} M) forms a gel in DMF/benzylalcohol 1:3 (*v*/*v*), the spectral shape is significantly broadened and the Soret band shifts to a shorter wavelength, whereas the Q bands shift to a longer wavelength. The same tendency is observed for **1b** (3.9×10^{-3} M) and **1c** (3.9×10^{-3} M). These shifts imply the presence of a H-aggregation mode in the porphyrin–porphyrin stacking array.[16] Shoulder-like absorption patterns are observed around 430 nm in all spectra for **1a–c**. It is probable that the gelator concentration is near the CGC, so that some gelator molecules that do not participate in the formation of the one-dimensional structure still remain.

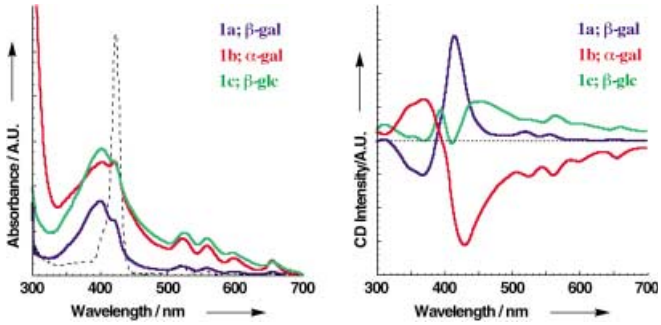

Figure 1. UV-Vis (left) and CD (right) spectra of the gels: blue; **1a**, red; **1b**, and green; **1c** (DMF/benzylalcohol 1:3 (*v*/*v*)), [**1a–c**] = 7.0 g dm^{-3} (25 °C), and dotted line; homogeneous solution of **1a** (DMF/benzylalcohol 1:2 (*v*/*v*), [**1a**] = 2.3×10^{-6} M (25 °C).

LD and CD spectroscopic analyses: To characterize the aggregation mode in the organogel phase, we examined the CD (circular dichroism) spectra of the **1a–c** gels. Figure 1 shows that the CD band for **1a** can be assigned to the positive exciton coupling and is observed only in the gel phase. This indicates that, as already observed for cholesterol-appended porphyrin gelators,[12] the one-dimensional porphyrin column is helically twisted under the influence of sugar chirality. Symmetric CD spectra were observed for **1a** and **1b** whose molecular skeletons were in anomers. The gel from **1c** gives a different CD spectral pattern, which suggests that the aggregation mode is different from that of **1a** and **1b**. We confirmed that the contribution of linear dichroism (LD) to the true CD spectrum is negligible by using the conventional LD mode. Also, we have excluded the possibility of intramolecular induced CD from the chiral sugar-moieties to the achiral porphyrin core, since the DMF solution of **1a** (2.3×10^{-6} M) is CD-silent.

Scanning electron microscopy (SEM): To obtain visual insights into the aggeregation mode of the gelators in the gel fibrils, we observed the SEM images of the xerogels prepared from **1a–c**. Figure 2 shows the SEM pictures of the xerogels obtained from DMF–benzylalcohol mixed solvents.

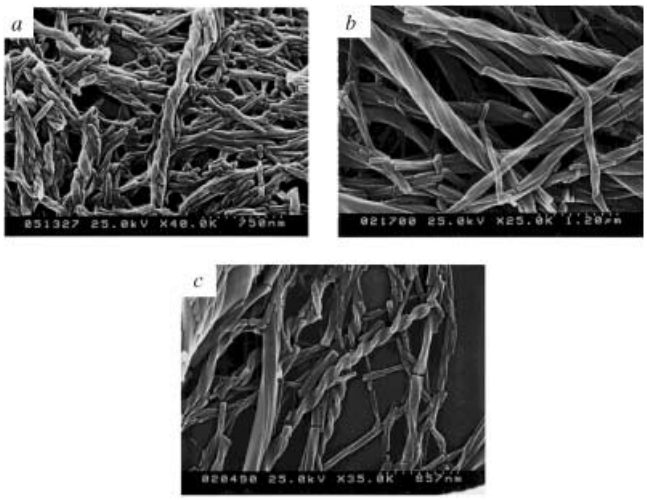

Figure 2. SEM images of the xerogels of a) **1a** partial gel (DMF/benzylalcohol 1:3 (*v*/*v*), [**1a**] = 4.0 g dm^{-3}), b) **1b** gel (DMF/benzylalcohol 1:2 (*v*/*v*), [**1b**] = 17 g dm^{-3}), and c) **1c** gel (DMF/benzylalcohol 1:2 (*v*/*v*), [**1c**] = 7.0 g dm^{-3}).

The xerogel **1a** mainly consists of three-dimensional tangling fiber-like aggregates with diameters of 200–300 nm (see Figure 2a).[13] A clear helical structure of **1a** is observed in the SEM image when the xerogel was prepared from **1a** of DMF/benzylalcohol 1:3 (*v*/*v*) mixed solvent at the concentration of 4.0 g dm^{-3}. Importantly, one can recognize a left-handed helical structure in the gel fibers of **1a** in Figure 2a. This gel gives the positive sign of the exciton coupling in the CD spectrum (Figure 1). In contrast, one can recognize a right-handed helical structure in the gel fibers of **1b** in Figure 2b. This gel gives the negative sign of the exciton coupling in the CD spectrum, which is a symmetrical pattern to that of **1a**. As shown in Figure 2c, the xerogel of **1c** gives both a helical structure (left-handed) and a flat sheet-like structure. These results qualitatively support the view, that the helical sense of the gel fibers is profoundly associated with the CD sign.

An interesting observation is seen from the supernatant of the samples, in which fine fibrils are tied into the bundle with the left-handed helices (Figure S3a and S3b in the Sup-

porting Information). This "baby-fibril" gives crucial evidence that thin fibrils are tied up into the bundles even in the solution state. The same image of the intermediate was also seen in the TEM (transition electron microscopy) image of the xerogel prepared from **1a** (30 g dm^{-3}, DMF/benzylalcohol 1:2 (*v*/*v*)) (Figure S3c in the Supporting Information).

Sol–gel transcription in sugar-appended porphyrin gels: Sol–gel polycondensation of TEOS was performed in **1a**+DMF–benzylalcohol gel according to the method described previously.[14] For example, **1a** (4.0 mg) was dissolved by heating at 80 °C into a mixture of DMF (160 mL), benzylalcohol (480 mL), and TEOS (35 mL). When this solution was cooled to room temperature, it gelled. Before the gel was formed, benzylamine (10 mL) and water (10 mL) were added. In Method A, the mixture was heated at 80 °C again and then left at room temperature for two weeks. On the other hand, in Method B, the mixture was just left at room temperature without heating. Therefore, the silica gel obtained was washed with methanol to remove organic compounds that adsorbed on the silica outer surface. After this treatment, the sample obtained by Method A was subjected to XPS (X-ray photelectron spectroscopy) analysis to obtain information on the silica outer surface. The N peak at 409 eV, which resulted from **1a** or benzylamine, was very weak, and the relative intensity against the Si peak at 112 eV was 8:92. This result shows that **1a** is scarcely adsorbed on the silica outer surface.

When **1a** (3.3×10^{-3} M) forms a gel in DMF/benzylalcohol/benzylamine 40:120:3 (*v*/*v*/*v*), the UV/Vis spectral shape is significantly broadened and the Soret bands shift to a shorter wavelength (397 nm), whereas the Q bands shift to a longer wavelength (524, 559, 600, and 656 nm). This spectral change, relative to the monomer solution of **1a**, supports the porphyrin–porphyrin stacking interaction in the assembly of **1a**.[16] The absorption spectrum after sol–gel polycondensation of **1a** (Method A) is interesting. Both the Soret and the Q bands appear at nearly the same wavelengths as those of the organogel phase (Figure 3a). The result implies that the stacked porphyrin structure is still retained in the silica gel-phase.[16] This view is further supported by the CD spectra, as shown in Figure 3b, the CD spectrum obtained after sol–gel polycondensation is very similar to that obtained from the organogel phase.

To obtain visual insights into the silica structure directly, we observed SEM and TEM images before and after calcination. The silica obtained by Method A from **1a** before calcination shows the fibrous structure to have an outer diameter of about 50 nm (Figure 4a). This morphology was scarcely changed even after calcination; this is seen from the SEM image of the sample after calcination at 500 °C (Figure 4b). The TEM images are shown in Figure 4c–e. It is clearly seen that these silica fibers have an inner hollow with 4~12 nm diameters. Careful observation reveals that there are two different hollow diameters, one being about 5 nm, comparable to a long-axis size of **1a** (4.2 nm: Figure 4d), and another being about 9 nm comparable to the double of the long-axis size, and bears a stripe in the center (Figure 4e). The TEM images are scarcely changed even after calcination, but the central stripe in Figure 4e disappeared.

In Method A, the solution which contains benzylamine (polycondensation catalyst)[14] was heated so that the bundle formation of organogel fibers was suppressed, while the rate of sol–gel polycondensation of TEOS was accelerated. Obviously, this condition facilitates the entrapment of incipient organogel fibers, which consist of a uni- or bimolecular stack. When the solution was not heated after benzylamine addition (Method B), the bundle growth of organogel fibers could compete with sol–gel polycondensation; this resulted in a helically-bundled silica structure as a result of transcription of well-grown, right- or left-handed, helically bundled organogel fibers of **1a–c** (Figure 5).

The foregoing results consistently support the view that **1a** aggregates in a one-dimensional stack, along which sol–gel polycondensation of TEOS proceeds in the gel phase. The size of the inner hollow in Method A suggests that the incipient organogel fibers are encapsulated in these silica hollow-fibers. The disappearance of the central stripe upon calcination is rationalized in terms of the disappearance of stacked **1a** molecules by pyrolysis. In addition, **1b** and **1c** gel fibrils also act as templates for the sol–gel transcription of μm-scale helical bundles.

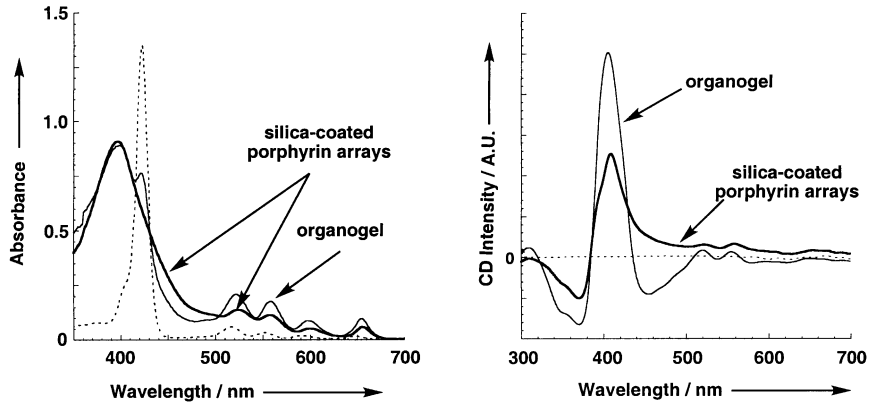

Figure 3. Absorption (left) and CD (right) spectra of silica-coated porphyrin arrays (bold line), organogel of **1a** (thin line), and homogeneous solution of **1a** (broken line; [**1a**] = 2.3×10^{-6} M).

Conclusion

To conclude, the present study has demonstrated that sugar-appended porphyrin derivatives that are rationally designed towards the construction of one-dimensional architechtures act as excellent gelators for very specific solvent mixtures. Although one-dimensional alignment of porphyrins has been attained in liquid- [1] and bulk-crystal systems,[2,17] no such precedent exists in an organo-

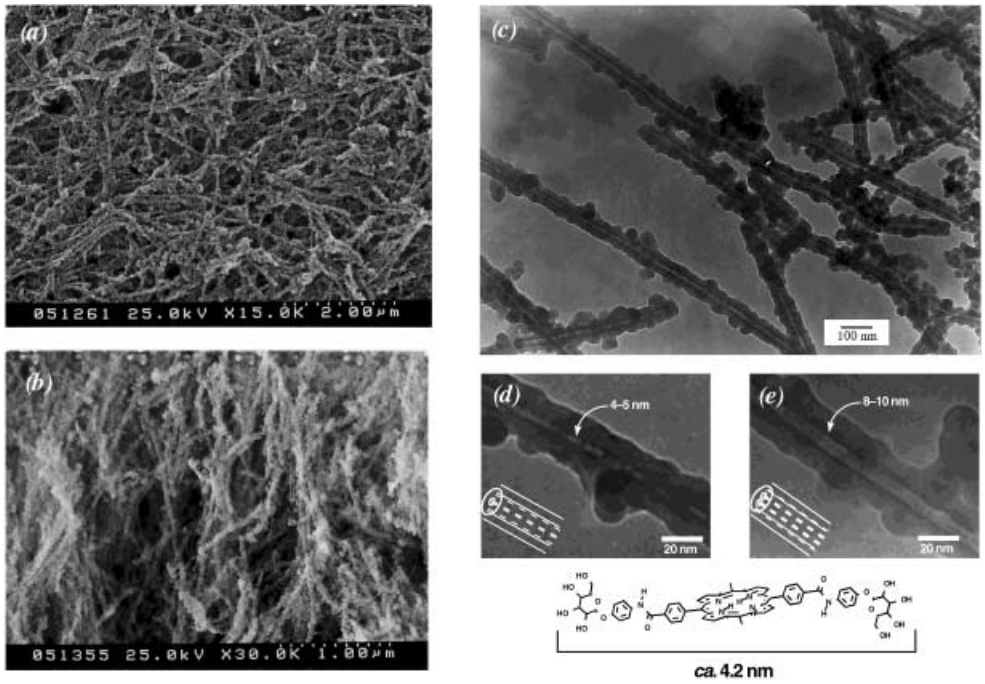

Figure 4. SEM (left) and TEM (right) images of silica-coated porphyrin arrays prepared by method A: a) before calcination and b)–e) after calcination.

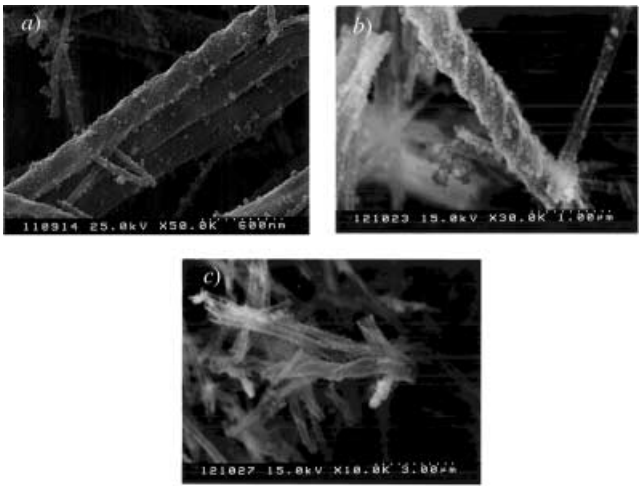

Figure 5. SEM images of the silica structure prepared by method B: a) **1a**, b) **1b**, and c) **1c** gel fibrils as a template (before calcination).

gel system. The organogel system, which is different from liquid- and bulk-crystal systems, both feature thermo- and lyotropic characteristics, which are conveniently used to append the switch function and the self-assembling function to the one-dimensional porphyrin stack. In addition, the helical direction and pitch can be finely tuned by combinatorial displacement of saccharide groups available from a natural library of carbohydrate molecules.

By using the porphyrinic fiber library, nm level sol–gel transcription of organic assemblies has been achieved when the incipient organic assembly is stable in the gel phase, and the sol–gel reaction conditions are appropriately selected. So far, the silica superstructures obtained by template transcription of organic assemblies have been characterized by the broad size distribution. This polydispersed nature has made their chemical applications difficult. We thus believe that the creation of the new silica fiber structure with the nearly monodispersed hollow size is very essential and applicable to other related transcription systems. For example, the nano-sized hollow will be useful as a host cavity to enforce molecules to orientate into a one-dimensional direction. This suggests there is future potential to create various nano-sized cavities by designing various sizes of "organic" template molecules. Without a doubt, it is therefore worthy to emphasize this feature of this sol–gel transcription method.

Experimental Section

General: All melting points were uncorrected. ^{1}H and ^{13}C NMR spectra were measured on a Brucker DMX 600 apparatus with tetramethylsilan as the internal standard. Optical rotations were measured on a Horiba SEPA-300. ATR-IR spectra were obtained by using a Perkin–Elmer Instruments Spectrum One FT-IR spectrometer. MALDI-TOF MS spectra were obtained by PerSeptive Biosystems Voyager-DE RP Biospecteometry Workstation. UV/Vis, CD (LD), and X-ray photoelectron spectra were recorded on a Shimadzu UV-2500PC spectrophotometer, a JASCO J-720 spectrometer, and a Perkin–Elmer ESCA 5300 spectrometer, respectively.

Gelation test: The gelator and the solvent were put in a screw-capped test-tube and heated until the solid was dissolved. The solution was cooled to room temperature and turned upside down. If the gelator formed a stable gel by immobilizing the solvent at this stage, it was denoted as G in Table 1.

Estimation of gel–sol phase transition temperature (T_{gel}): A test tube that contained the gel was horizontally immersed in a thermo-controlled oil bath. The temperature was raised at 2.0 °C min^{-1}. The T_{gel} was defined as the temperature at which the gel changed to a liquid.

SEM measurements: A Hitachi S-5000 scanning electron microscope was used for taking the SEM images. A thin gel, which was prepared in a

sample tube, was freeze-dried by a vacuum pump at −10 °C. The dried sample obtained was shielded by Pt. The accelerating voltage of SEM was 25 kV.

TEM measurements: A piece of the dried gel sample which was prepared for SEM observation was placed on a carbon-coated copper grid (200 mesh). After the sample was stained by one drop of an aqueous solution of phosphotungstic acid (2.0 % wt), the specimen was dried in vacuo, and the sample was examined with a Hitachi H-600 TEM (acceleration voltage: 75 kV) to obtain TEM images.

Sol–gel polycondensation method A: Gelator (4.0 mg) was added to a mixed solvent of DMF (160 mL) and benzylalcohol (480 mL), and the mixture was heated until the precipitate completely dissolved. Tetraethylorthosilicate (TEOS 35 mL), benzylamine (10 mL), and water (10 mL) was then added to this mixture. The reaction mixture was then heated until it became homogeneous, and then placed at room temperature in the dark for two weeks. The product was washed with methanol and dried in vacuo to give the organic-inorganic composite as a purple solid. This sample was calcinated to remove gelators at 150 °C for 2 h and 500 °C for 5 h, under a nitrogen stream, and at 500 °C for 5 h under an aerobic stream. The silica obtained was colorless.

Sol–gel polycondensation method B: Gelator (1.0 mg) was added to a mixture of DMF (40 mL), benzylalcohol (120 mL), and TEOS (10 mL), and the resultant mixture was heated until the precipitate completely dissolved . After this mixture was cooled to room temperature, benzylamine (3.0 mL) and water (3.0 mL) were added. Without the heating process, this reaction mixture was placed at room temperature in the dark for two weeks. The product was washed with methanol, and dried in vacuo to give the organic-inorganic composite as a purple solid.

Preparation of 1a: A mixed solution of **5a** (0.94 g, 0.38 mmol), sodium methoxide (0.1 M in methanol, 3.0 mL) was added to dry methanol (20 mL) and dry tetrahydrofuran (6.0 mL), and the mixture was stirred for 1.5 h under nitrogen. After the removal of the solvent under reduced pressure, the purple solid was washed by chloroform and purified by reprecipitation to give **1a** (0.55 g, 0.30 mmol, 76 %). M.p. 236–237 °C; ^{1}H NMR (600 MHz, [D$_6$]DMSO): $\delta = -2.87$ (s, 2H), 3.45–3.58 (m, 16H; H$_3$, H$_4$, H$_5$, H$_6$, H$_6'$), 3.73–3.74 (m, 4H; H$_2$), 4.54–5.22 (m, 16H; OH$_2$, OH$_3$, OH$_4$, OH$_6$), 4.85 (d, J = 7,5 Hz, 4H; H$_1$), 7.12 (d, J = 8.8 Hz, 8H; Ar-H), 7.84 (d, J = 8.8 Hz, 8H; Ar-H), 8.41–8.42 (m, 16H; Ar-H), 8.93 (s, 8H; β-pyrrole), 10.6 ppm (m, 4H; amide-NH); ^{13}C NMR (150 MHz, [D$_6$]DMSO): δ = 60.629 (CH$_2$), 68.378 (CH), 70.551 (CH), 73.557 (CH), 75.720 (CH), 101.600 (CH), 116.679 (CH), 119.696 (Cq), 122.113 (CH), 126.508 (CH), 133.585 (Cq), 134.423 (CH), 134.869 (Cq), 144.339 (Cq), 154.109 (Cq), 165.371 ppm (C=O); ATR-IR: $\tilde{\nu}$ = 3314, 1645, 1606, 1507, 1216, 1048, 1019 cm^{-1}; UV/Vis (DMF): λ_{max} (ε) = 420.0 (381000), 515.0 (17900), 549.5 (10000), 590.0 (6050), 646.5 (5200 mol^{-1}dm^{3}cm^{-1}) nm; MALDI-TOF MS (matrix: dithranol): calcd m/z for $[M+H]^+$: 1805.78; found 1804.28. elemental analysis calcd (%) for $C_{96}H_{90}N_8O_{28}$·4 CH_3OH: C 62.17, H 5.53, N 5.80; found C 62.18, H 5.31, N 5.93. The same procedure was applied for the preparation of **1b–e**. We thus only recorded their analytical data.

Preparation of 1b: Compound **5b** (1.1 g, 0.44 mmol) was deprotected with sodium methoxide to give **1b** (0.63 g, 0.35 mmol, 74 %). M.p. 239–243 °C decomp; ^{1}H NMR (600 MHz, [D$_6$]DMSO): $\delta = -2.88$ (s, 2H), 3.41–3.59 (m, 8H; H$_6$, H$_6'$), 3.77–3.82 (m, 16H; H$_2$, H$_3$, H$_4$, H$_5$), 4.54–4.90 (m, 16H; OH$_2$, OH$_3$, OH$_4$, OH$_6$), 5.40–5.41 (m, 4H; H$_1$), 7.15 (d, J = 8.9 Hz, 8H; Ar-H), 7.82 (d, J = 8.9 Hz, 8H; Ar-H), 8.40–8.42 (m, 16H; Ar-H), 8.92 (s, 8H; β-pyrrole), 10.6 ppm (s, 4H, amide-NH); ^{13}C NMR (150 MHz, [D$_6$]DMSO): δ = 60.527 (CH$_2$), 68.273 (CH), 68.735 (CH), 69.673 (CH), 72.415 (CH), 98.829 (CH), 117.478 (CH), 119.681 (Cq), 122.094 (CH), 122.271 (Cq), 126.507 (CH), 133.660 (Cq), 134.384 (CH), 134.849 (Cq), 144.320 (Cq), 153.855 (Cq), 165.336 ppm (C=O); ATR-IR: ν = 3316, 1651, 1606, 1509, 1216, 1076, 1026 cm^{-1}; UV/Vis (DMF): λ_{max} (ε) = 420.0 (494000), 515.0 (21700), 549.5 (11700), 590.0 (6770), 646.5 nm (6170 mol^{-1}dm^{3}cm^{-1}); MALDI-TOF MS (matrix: dithranol): calcd m/z for $[M+H]^+$: 1805.78; found 1805.20. elemental analysis calcd for $C_{96}H_{90}N_8O_{28}$·0.65 CH_3OH: C 63.62, H 5.12, N 6.14; found C 63.49, H 4.97, N 6.19.

Preparation of 1c: Compound **5c** (1.3 g, 0.52 mmol) was deprotected with sodium methoxide to give **1c** (0.62 g, 0.34 mmol, 62 %). M.p. 236 °C; ^{1}H NMR (600 MHz, [D$_6$]DMSO): $\delta = -2.88$ (s, 2H), 3.17–3.75 (m, 16H; H$_2$, H$_3$, H$_4$, H$_5$), 3.48–3.75 (m, 8H; H$_6$, H$_6'$), 4.61–4.63 (m, 4H; OH$_6$), 4.88 (d, J = 7.3 Hz, 4H; H$_1$), 5.04–5.37 (m, 12H; OH$_2$, OH$_3$, OH$_4$), 7.11 (d, J = 8.9 Hz, 8H; Ar-H), 7.83 (d, J = 8.9 Hz, 8H; Ar-H), 8.40–8.41 (m, 16H; Ar-H), 8.92 (s, 8H; β-pyrrole), 10.6 ppm (s, 4H; amide-NH); ^{13}C NMR (150 MHz, [D$_6$]DMSO): δ = 60.527 (CH$_2$), 69.986 (CH), 73.505 (CH), 76.889 (CH), 77.273 (CH), 101.097 (CH), 116.682 (CH), 119.695 (Cq), 122.126 (CH), 122.558 (Cq), 126.607 (CH), 133.669 (Cq), 134.871 (CH), 144.342 (Cq), 154.028 (Cq), 165.392 ppm (C=O); ATR-IR: $\tilde{\nu}$ = 3279, 1646, 1607, 1506, 1217, 1038, 1014 cm^{-1}; UV/Vis (DMF): λ_{max} (ε) = 420.0 (316000), 515.0 (17100), 549.5 (10200), 590.0 (6590), 646.0 nm (5330 mol^{-1}dm^{3}cm^{-1}); MALDI-TOF MS (matrix: dithranol): calcd m/z for $[M+H]^+$: 1805.78; found 1805.23: elemental analysis calcd for $C_{96}H_{90}N_8O_{28}$·1.8 CH_2Cl_2: C 60.03, H 4.92, N 5.73; found: C 59.73, H 5.20, N 5.52.

Preparation of 1d: Compound **5d** (0.58 g, 0.42 mmol) was deprotected with sodium methoxide to give **1d** (0.58 g, 0.32 mmol, 70 %). M.p. 240–242 °C; ^{1}H NMR (600 MHz, [D$_6$]DMSO): $\delta = -2.89$ (s, 2H), 3.47–3.53 (m, 12H; H$_4$, H$_5$, H$_6$), 3.63 (d, J = 11 Hz, 4H; H$_3$, H$_6'$), 3.70–3.71 (m, 4H; H$_3$), 3.85–3.86 (m, 4H; H$_2$), 4.51–5.04 (m, 16H; OH$_2$, OH$_3$, OH$_4$, OH$_6$), 5.38 (s, 4H; H$_1$), 7.16 (d, J = 9 Hz, 8H; Ar-H), 7.83 (d, J = 9 Hz, 8H; Ar-H), 8.40–8.41 (m, 16H; Ar-H), 8.92 (s, 8H; β-pyrrole), 10.6 ppm (s, 4H; amide-NH); ^{13}C NMR (150 MHz, [D$_6$]DMSO): δ = 61.318 (CH$_2$), 69.996 (CH), 70.295 (CH), 70.928 (CH), 75.125 (CH), 99.542 (CH), 117.316 (CH), 119.677 (Cq), 122.102 (CH), 126.500 (CH), 133.836 (Cq), 134.374 (CH), 134.850 (Cq), 144.47 (Cq), 152.934 (Cq), 165.367 ppm (C=O); ATR-IR: $\tilde{\nu}$ = 3314, 1652, 1606, 1508, 1217, 1005 cm^{-1}; UV/Vis (DMF): λ_{max} (ε) = 420.5 (130000), 515.0 (9040), 549.0 (6170), 591.0 (4730), 645.5 nm (4130 mol^{-1}dm^{3}cm^{-1}); MALDI-TOF MS (matrix: dithranol): calcd m/z for $[M+H]^+$: 1805.78 (1805.23): elemental analysis calcd (%) for $C_{96}H_{90}N_8O_{28}$·0.90 CH_3OH: C 63.51, H 5.15, N 6.11; found C 63.29, H 4.93, N 6.21.

Preparation of 1e: Compound **5e** (0.58 g, 0.23 mmol) was deprotected with sodium methoxide to give **1e** (0.32 g, 0.18 mmol, 74 %). M.p. 218 °C; ^{1}H NMR (600 MHz, [D$_6$]DMSO): $\delta = -2.87$ (s, 2H), 3.51–3.57 (m, 12H; H$_4$, H$_5$, H$_6$), 3.67–3.75 (m, 8H; H$_3$, H$_6'$), 3.89–3.90 (m, 4H; H$_2$), 4.53–5.07 (m, 16H; OH$_2$, OH$_3$, OH$_4$, OH$_6$), 5.68–5.69 (m, 4H; H$_1$), 7.19–7.21 (m, 8H; Ar-H), 7.34–7.36 (m, 4H; Ar-H), 8.33–8.34 (m, 4H; Ar-H), 8.42–8.45 (m, 16H; Ar-H), 8.96 (s, 8H; β-pyrrole), 9.94 ppm (s, 4H; amide-NH); ^{13}C NMR (150 MHz, [D$_6$]DMSO): δ = 60.654 (CH$_2$), 68.337 (CH), 70.767 (CH), 73.115 (CH), 76.082 (CH), 104.113 (CH), 118.358 (CH), 119.622 (Cq), 122.171 (CH), 123.365 (CH), 125.022 (CH), 126.426 (CH), 129.608 (CH), 134.241 (Cq), 134.751 (CH), 144.681 (Cq), 148.231 (Cq), 154.158 (Cq), 165.131 ppm (C=O); ATR-IR: $\tilde{\nu}$ = 3314, 1647, 1602, 1248, 1048 cm^{-1}; UV/Vis (DMF): λ_{max} (ε) = 420.5 (428000), 515.5 (22000), 550.0 (13500), 590.5 (8800), 646.5 nm (7960 mol^{-1}dm^{3}cm^{-1}); FAB MS (HR): calcd m/z for $C_{96}H_{90}N_8O_{28}$: 1802.5865; found 1802.5852.

Acknowledgement

We thank Ms. Hongyue Li for the measurements of NMR spectra. The present work was supported by a Grant-in-Aid for the 21st Century COE Program, "Functional Innovation of Molecular Informatics" from the Ministry of Education, Culture, Science, Sports and Technology of Japan.

[1] a) C. F. van Nostrum, S. J. Picken, A.-J. Schouten, R. J. M. Nolte, *J. Am. Chem. Soc.* **1995**, *117*, 9957–9965; b) A. P. H. Schenning, F. B. G. Benneker, H. P. M. Geurts, X. Y. Liu, R. J. M. Nolte, *J. Am. Chem. Soc.* **1996**, *118*, 8549–8552; c) C. F. van Nostrum, R. J. M. Nolte, *Chem. Commun.* **1996**, 2385–2392; d) H. Engelkamp, C. F. van Nostrum, S. J. Picken, R. J. M. Nolte, *Chem. Commun.* **1998**, 979–980; e) H. Engelkamp, S. Middelbeek, R. J. M. Nolte, *Science* **1999**, *284*, 785–788; f) S. Samori, H. Engelkamp, P. de Witte, A. E. Rowan, R. J. M. Nolte, J. P. Rabe, *Angew. Chem.* **2001**, *113*, 2410–2412; *Angew. Chem. Int. Ed.* **2001**, *40*, 2348–2350, and references therein.

[2] a) J.-H. Fuhrhop, C. Demoulin, C. Boettcher, J. Koning, U. Siffel, *J. Am. Chem. Soc.* **1992**, *114*, 4159–4165; b) J.-H. Fuhrhop, U. Bindig,

U. Siggel, *J. Am. Chem. Soc.* **1993**, *115*, 11036 – 11037; c) U. Bindig, A. Schulz, J.-H. Fuhrhop, *New J. Chem.* **1995**, *19*, 427 – 435, and references therein.

[3] a) P. Smolenyak, R. Peterson, K. Nebesny, M. Torker, D. F. O'Brien, N. R. Armstrong, *J. Am. Chem. Soc.* **1999**, *121*, 8628 – 8636; b) S. A. Drager, R. A. P. Zangmeister, N. R. Armstrong, D. F. O'Brien, *J. Am. Chem. Soc.* **2001**, *123*, 3595 – 3596.

[4] a) M. Kimura, T. Kitamura, T. Muto, K. Hanabusa, H. Shirai, N. Kobayashi, *Chem. Lett.* **2000**, 1088 – 1089; b) M. Kimura, T. Muto, H. Takimoto, K. Wada, K. Ohta, K. Hanabusa, K. H. Shirai, N. Kobayashi, *Langmuir* **2000**, *16*, 2078 – 2082; c) M. Kimura, K. Wada, K. Ohta, K. Hanabusa, H. Shirai, N. Kobayashi, *J. Am. Chem. Soc.* **2001**, *123*, 2438 – 2439.

[5] a) T. Imada, H. Murakami, S. Shinkai, *Chem. Commun.* **1994**, 1557 – 1558; b) S. Arimori, M. Takeuchi, S. Shinkai, *J. Am. Chem. Soc.* **1996**, *118*, 245 – 246; c) S. Arimori, M. Takeuchi, S. Shinkai, *Supramol. Sci.* **1998**, *5*, 1 – 8.

[6] R. Luboradzki, O. Gronwald, M. Ikeda, S. Shinkai, D. N. Reinhoudt, *Tetrahedron* **2000**, *56*, 9595 – 9599.

[7] For comprehensive reviews for organogels, see a) J. van Esch, F. Schoonbeek, M. de Loos, H. Kooijman, E. M. Veen, R. M. Kellogg, B. L. Feringa, In *Supramolecular Science: Where It Is and Where It Is Going* (Eds.: R. Ungaro, E. Dalcanale), Kluwar, Dordewcht, **1999**, p 233 – 259; b) R. E. Melendez, A. J. Carr, B. R. Linton, A. D. Hamilton, *Struct. Bonding* **2000**, *96*, 31 – 61; c) S. Shinkai, K. Murata, *J. Mater. Chem.* **1998**, *8*, 485 – 495.

[8] a) K. Yoza, Y. Ono, K. Yoshihara, T. Akao, H. Shinmori, M. Takeuchi, S. Shinkai, D. N. Reinhoudt, *Chem. Commun.* **1998**, 907 – 908; b) K. Yoza, N. Amanokura, Y. Ono, T. Akao, H. Shinmori, S. Shinkai, D. N. Reinhoudt, *Chem. Eur. J.* **1999**, *5*, 2722 – 2729; c) N. Amanokura, K. Yoza, H. Shinmori, S. Shinkai, D. N. Reinhoudt, *J. Chem. Soc. Perkin Trans. 2* **1998**, 2585 – 2591; d) O. Gronwald, K. Sakurai, R. Luboradzki, T. Kimura, S. Shinkai, *Carbohydr. Res.* **2001**, *331*, 307 – 318.

[9] For a comprehensive review for sugar-based gelators, see O. Gronwald, S. Shinkai, *Chem. Eur. J.* **2001**, *7*, 4328 – 4334.

[10] R. Luboradzki, O. Gronwald, A. Ikeda, S. Shinkai, *Chem. Lett.* **2000**, 1148 – 1149.

[11] The tetrakis(*O*-tetraacetyl) derivative of **1** was very soluble in most organic solvents and did not act as a gelator. The similar porphyrin derivatives were synthesized by Fuhrhop's group (ref. [2]), but they were not applied to the organogel system. Recently, Stoddart et al. synthesized sugar-coated discotic liquid crystals bearing a triphenylene core and porphyrin-containing glycodendrimers. The gelation properties were not examined therein: a) J. Barbera, A. C. Garces, N. Jayaraman, Omenat, J. L. Serrano, J. F. Stoddart, *Adv. Mater.* **2001**, *13*, 175 – 180; b) R. Ballardini, B. Colonna, M. T. Gandolfi, S. A. Kalovidouris, L. Orzel, F. M. Raymo, J. F. Stoddart, *Eur. J. Org. Chem.* **2003**, 288 – 294.

[12] A preliminary communication: a) S.-i. Tamaru, M. Takeuchi, M. Sano, S. Shinkai, *Angew. Chem.* **2002**, *114*, 881 – 884; *Angew. Chem. Int. Ed.* **2002**, *41*, 853 – 856; we also found that certain cholesterol-appended porphyrins act as gelators of organic solvent: b) T. Ishi-i, J. H. Jung, S. Shinkai, *J. Mater. Chem.* **2000**, *10*, 2238 – 2240; c) H. J. Tian, K. Inoue, K. Yoza, T. Ishi-i, S. Shinkai, *Chem. Lett.* **1998**, 871 – 872. In these organogels, however, it is considered that porphyrin moieties are located around a helical central column of cholesterol moieties, like a spiral staircase.

[13] S.-i. Tamaru, M. Nakamura, M. Takeuchi, S. Shinkai, *Org. Lett.* **2001**, *3*, 3631 – 3634.

[14] a) Y. Ono, K. Nakashima, M. Sano, Y. Kanekiyo, K. Inoue, J. Hojo, S. Shinkai, *Chem. Commun.* **1998**, 1477; b) Y. Ono, K. Nakashima, M. Sano, J. Hojo, S. Shinkai, *Chem. Lett.* **1999**, 1119; c) J. H. Jung, Y. Ono, S. Shinkai, *Angew. Chem.* **2000**. *112*. 1931; *Angew. Chem. Int. Ed.* **2000**, *39*, 1862; d) J. H. Jung, Y. Ono, K. Hanabusa S. Shinkai, *J. Am. Chem. Soc.* **2000**, *122*, 5008; e) J. H. Jung, Y. Ono, S. Shinkai, *Chem. Eur. J.* **2000**, *6*, 4552; f) J. H. Jung, H. Kobayashi, M. Masuda, T. Shimizu, S. Shinkai, *J. Am. Chem. Soc.* **2001**, *123*, 8785; g) K. Sugiyasu, S.-i. Tamaru, M. Takeuchi, D. Berthier, I. Huc, R. Oda, S. Shinkai, *Chem. Commun.* **2002**, 1212. For the recent our review: K. J. C. van Bommel, A. Friggeri, S. Shinkai, *Angew. Chem.* **2003**, *115*, 1010 – 1030; *Angew. Chem. Int. Ed.* **2003**, *42*, 980 – 999.

[15] M. Amaike, H. Kobayashi, S. Shinkai, *Bull. Chem. Soc. Jpn.* **2000**, *73*, 2553 – 2558.

[16] K. Kano, K. Fukada, H. Wakami, R. Nishiyabu, R. F. Pasternack, *J. Am. Chem. Soc.* **2000**, *122*, 7494 – 7502.

[17] a) P. Bhyrappa, S. R. Wilson, K. S. Suslick, *J. Am. Chem. Soc.* **1997**, *119*, 8492 – 8502; b) P. Bhyrappa, S. R. Wilson, K. S. Suslick, *Supramol. Chem.* **1998**, *9*, 169 – 174; c) T. Tanaka, K. Endo, Y. Aoyama, *Bull. Chem. Soc. Jpn.* **2001**, *74*, 907 – 916.

Received: April 14, 2003
Revised: September 24, 2003 [F5042]

